

EVALUATION OF DEEP DRAWABILITY OF FLAME-RETARDANT MAGNESIUM ALLOY SHEETS

AKIHIRO MINAMI¹, HIROKAZU TAMURA², HIDETOSHI SAKAMOTO³, YOSHIFUMI OHBUCHI⁴ & YASUO MARUMO⁴

¹ National Institute of Technology, Ariake College, Japan.

² Graduate School of Science and Technology, Kumamoto University, Japan.

³ Department of Mechanical System Engineering, Doshisha University, Japan.

⁴ Faculty of Advanced Science and Technology, Kumamoto University, Japan.

ABSTRACT

The deep drawability of flame-retardant AMCa602 magnesium alloy sheets (aluminum, 6.5%; zinc, 0.08%, manganese, 0.32%; calcium, 2.1%) was investigated. Firstly, fundamental mechanical properties were obtained by performing uniaxial tension tests in the range of temperatures of 160–320°C. The tensile velocity was 0.5, 5 or 50 mm/min. Next, in deep-drawing tests, the temperature and punch velocity were changed, and a punch with a diameter of 10 mm was used. The experimental temperature was changed in the range from 240 to 340°C in increments of 20°C, and the punch velocity was 0.1, 0.5, 1.0 or 1.5 mm/s. Deep drawability improved as the temperature increased. The optimum deep-drawing temperature was found to be 320°C. A numerical simulation of deep drawing was conducted by finite element method for examining stress and strain distribution around breaking location. The experimental results and numerical simulation results were in relatively good agreement. A maximum deep-drawing depth was also obtained in the experiments and simulation.

Keywords: Deep Drawing, Flame-Retardant Mg Alloy, Formability, Mechanical Properties

1 INTRODUCTION

Magnesium alloy is the lightest structural metal and its specific gravity is approximately two-thirds that of aluminum. Additionally, they have good absorption of vibrations, high electromagnetic resistance, good machinability and good castability, and magnesium is an abundant natural resource. Magnesium alloys are useful in various applications including automobile parts, notebook computers and mobile electronic products. Magnesium alloys have been examined as next-generation materials to lighten transportation equipment. However, they have a low ignition temperature and burn easily. Furthermore, their ductility is poor at the room temperature [1]. The plastic formability of magnesium alloys is also very poor. Some magnesium alloy products are formed by die casting and thixotropic molding. In sheet metal forming, press forming is an important method for mass production. High formability is required to extend the range of applications of magnesium alloys, and both hot and warm forming are appropriate methods for achieving high formability [2]–[5]. In the previous paper [6], the formability of AZ31 magnesium alloy and flame-retardant magnesium alloy was discussed.

In this study, to promote the use of magnesium alloys by avoiding their disadvantages of poor formability and high flammability in press production, we examined the mechanical properties and deep drawability of flame-retardant AMCa602 magnesium alloy (aluminum 6.5%, zinc 0.08%, manganese 0.32%, calcium 2.1%) under hot and warm conditions in further detail. First, the effects of temperature and tensile velocity on the fundamental mechanical properties of AMCa602 were clarified in uniaxial tensile tests. Then hot and warm deep-drawing tests were conducted. The effects of the experimental temperature and experimental velocity on deep drawability were discussed. In addition, a finite element simulation of deep drawing was carried out using DEFORM-3D software.

2 EXPERIMENTAL CONDITIONS AND PROCEDURE

2.1 Tensile tests

Flame-retardant AMCa602 magnesium alloy sheets (NACHI-FUJIKOSHI CORP.) were used in this study. Table 1 shows the chemical composition of the used sheets. Uniaxial tensile tests of the material were conducted to obtain its mechanical properties. Table 2 shows the conditions of the uniaxial tensile tests. The velocity and temperature dependences of the mechanical properties were examined. The tensile velocity was 0.5, 5 or 50 mm/min and the experimental temperature was varied from 160°C to 320°C in increments of 20°C. Figure 1 shows the Autograph AG-25TB (SHIMADZU Corporation) used in the tensile tests. The tensile tester was equipped with a high temperature heating furnace

Table 1: Chemical composition of AMCa602.

Chemical component	Al	Zn	Mn	Fe	Si	Cu	Ni	Ca	Mg
Chemical composition (%)	6.5	0.08	0.32	<0.002	0.017	<0.002	0.002	2.1	Bal

Table 2: Uniaxial tensile test conditions.

Material	AMCa602 hot rolling sheet (t = 1.03mm)
Tensile velocity	0.5 mm/min, 5 mm/min, 50 mm/min
Directions	0°, 45°, 90°
Experimental temperature	160°C, 180°C, 200°C, 220°C, 240°C, 280°C, 300°C, 320°C, Room temperature

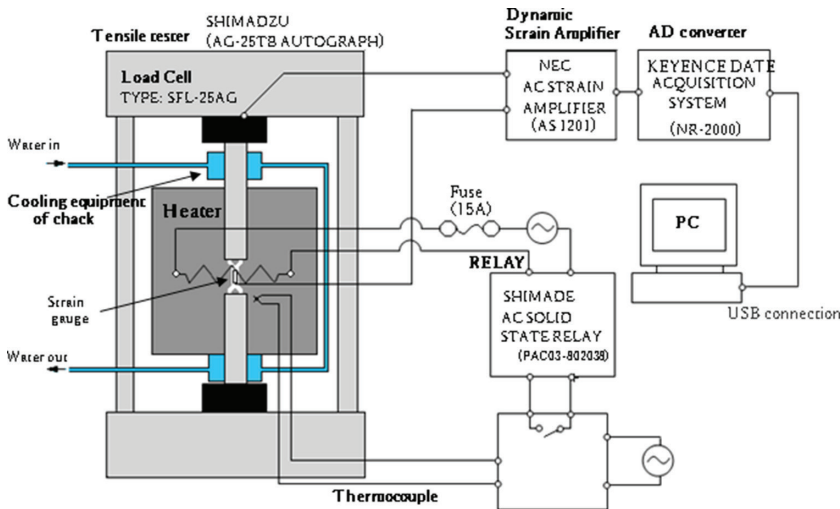


Figure 1: Schematic illustration of tensile test apparatus.

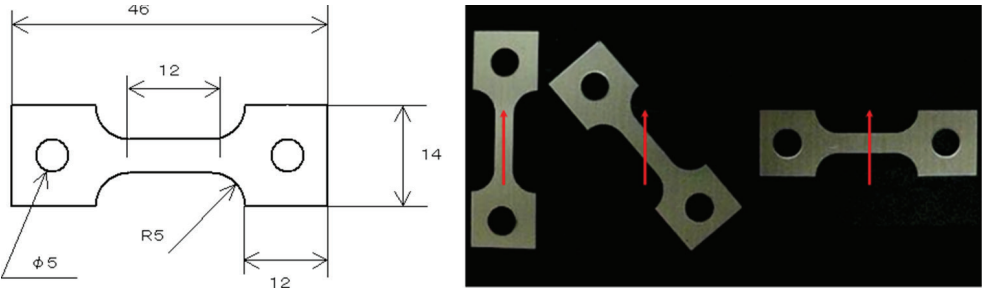


Figure 2: Geometry of tensile specimens.

whose temperature was maintained at the above temperatures during the tensile tests. Tensile specimens oriented at angles of 0°, 45° and 90° to the rolling direction were prepared as shown in Fig. 2.

2.2 Deep-drawing tests

Figure 3 shows the apparatus used for the deep-drawing tests. A cylindrical punch with a diameter of 10 mm was used. Table 3 shows the experimental conditions for the deep-drawing tests. To search for the optimal experimental conditions, deep-drawing tests were conducted while varying the temperature and velocity. Graphite was used for lubrication and circular specimens with a thickness of 1.0 mm were used.

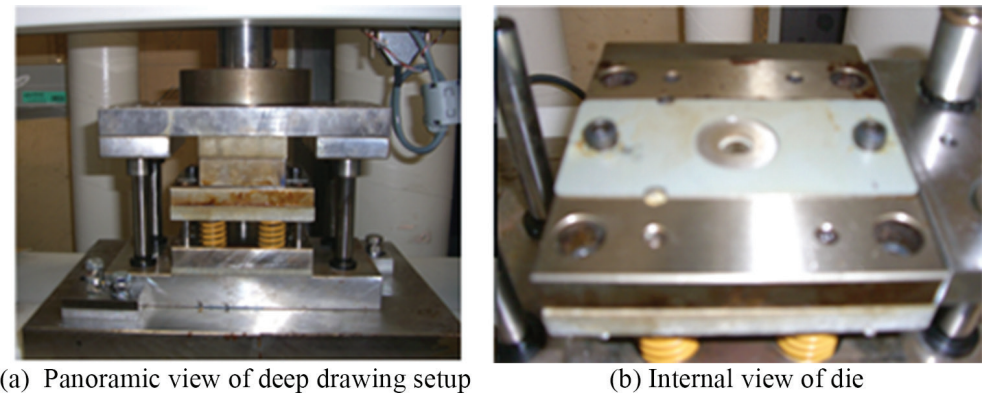


Figure 3: Deep drawing setup.

Table 3: Experimental conditions of deep drawing.

Specimen	Diameter 25 mm, Thickness 1.0 mm
Lubricant	Graphite
Temperature	240°C, 260°C, 280°C, 300°C, 320°C, 340°C
Experimental velocity	0.1 mm/s, 0.5 mm/s, 1.0 mm/s, 1.5 mm/s

3 EXPERIMENTAL RESULTS AND DISCUSSION

3.1 Mechanical properties of AMCa602 magnesium alloy sheets

Figures 4(a) and 4(b) show the variation in the tensile strength with the temperature for tensile velocities of 0.5 and 50 mm/min. Overall, the tensile strength tends to decrease with increasing temperature. Figure 5 shows the variation in the elongation with the temperature

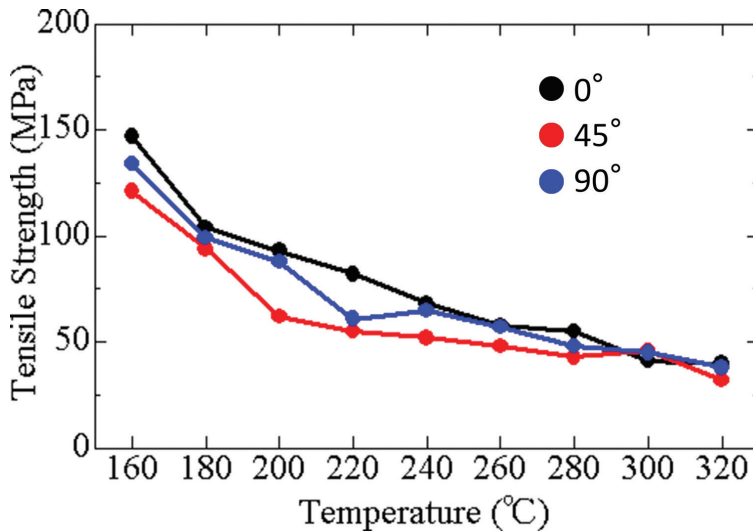


Figure 4(a): Variation in tensile strength with temperature (tensile velocity 0.5 mm/min).

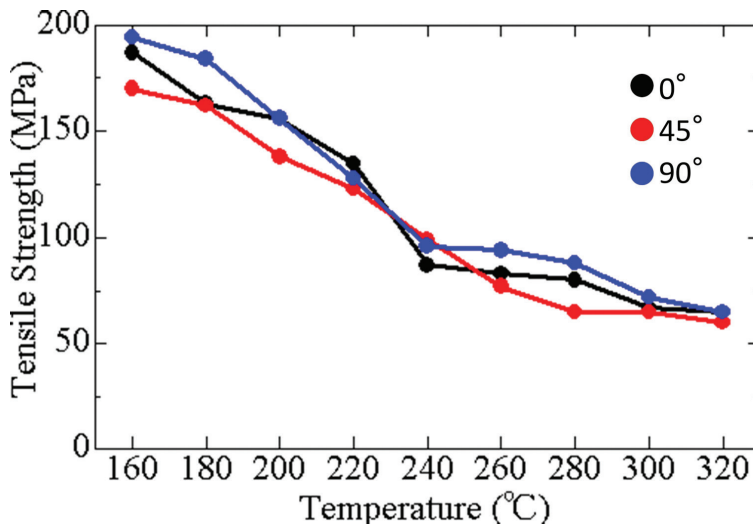


Figure 4(b): Variation in tensile strength with temperature (tensile velocity 50 mm/min).

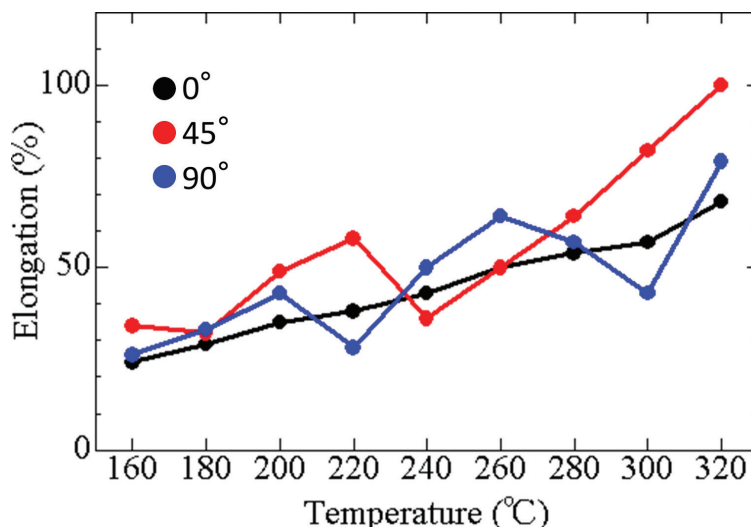


Figure 5: Variation in elongation with temperature (tensile velocity 50 mm/min).

for a tensile velocity of 50 mm/min. The elongation tends to increase with increasing temperature. Thus, it is expected that the deep drawability will be improved at high temperatures. A dependence of the tensile strength on the velocity was also confirmed: the tensile strength increased with increasing tensile velocity.

3.2 Results of deep-drawing tests

Figures 6 and 7 show photographs of deep-drawn cups shortly after reaching the maximum deep-drawing depth in the tests at 240°C and 340°C, respectively. The deep-drawn cups in the figures are arranged from left to right in order of increasing experimental velocity (punch velocity): (a) 0.1 mm/s, (b) 0.5 mm/s, (c) 1.0 mm/s and (d) 1.5 mm/s. At the lower temperature of 240°C (Fig. 6), cracks soon appeared on the punch shoulder (cup shoulder) and propagated to the cup wall. Such a fracture can be classified as localized fracture. At the higher temperature of 340°C (Fig. 7), cracks appeared on the punch shoulder (cup shoulder) relatively late and propagated circumferentially. Such a fracture can be classified as circumferential fracture. This fracture indicates that the deep-drawing force is sustained

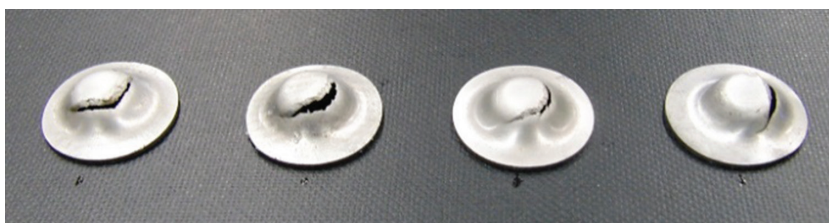


Figure 6: Specimens after deep drawing test (240°C). Experimental velocity (a) 0.1 mm/s, (b) 0.5 mm/s, (c) 1.0 mm/s, (d) 1.5 mm/s.



Figure 7: Specimens after deep-drawing test (340°C)
Experimental velocity (a) 0.1 mm/s, (b) 0.5 mm/s,
(c) 1.0 mm/s, (d) 1.5 mm/s.

circumferentially, resulting in a circumferentially uniform stress distribution. The fracture type indicates the uniformity of the stress and strain distributions in the area where cracks occur. These fracture types are roughly correlated with deep drawability. Figure 8 shows the variation in the maximum load with the temperature for each experimental velocity. The maximum load decreases with increasing temperature for all velocities because the flange material is softened. The maximum load at a high experimental velocity is higher than that at a low experimental velocity. This tendency corresponds to that of the tensile strength. Figures 9 and 10 show the relationships between the maximum deep-drawing depth and experimental velocity for 240°C, 260°C and 280°C and for 300°C, 320°C and 340°C, respectively. At high temperatures as shown in Fig. 10, a relatively large deep-drawing depth was obtained at an experimental velocity of 0.5 mm/s, whereas at low temperatures, as shown in Fig. 9, a large drawing depth was obtained at 1.0 mm/s. Figure 11 shows the variation in the maximum deep-drawing depth with temperature. Overall, the deep drawability was improved with increasing temperature. Compared with the deep drawability for 240°C, it was considerably improved at temperatures of 260°C and above. This is thought to be caused by twin crystals. At 340°C, the deep-drawing depth slightly decreased. This is considered to be attributable to an unstable structure formed by recrystallization. Thus, it was found that the optimum temperature was 320°C.

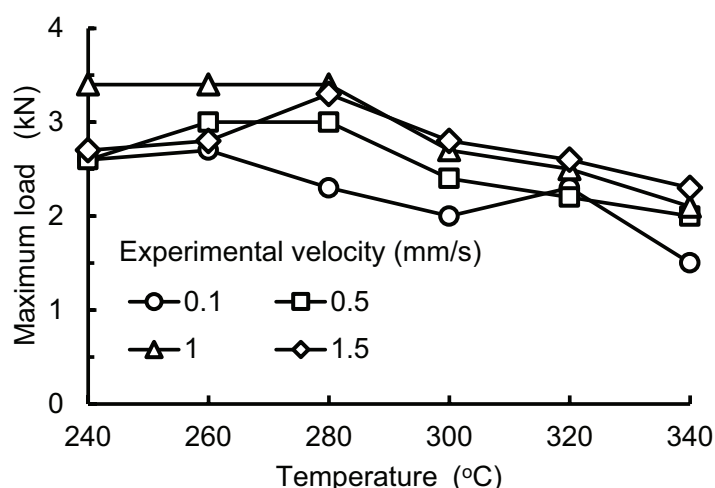


Figure 8: Variation in maximum load with temperature.

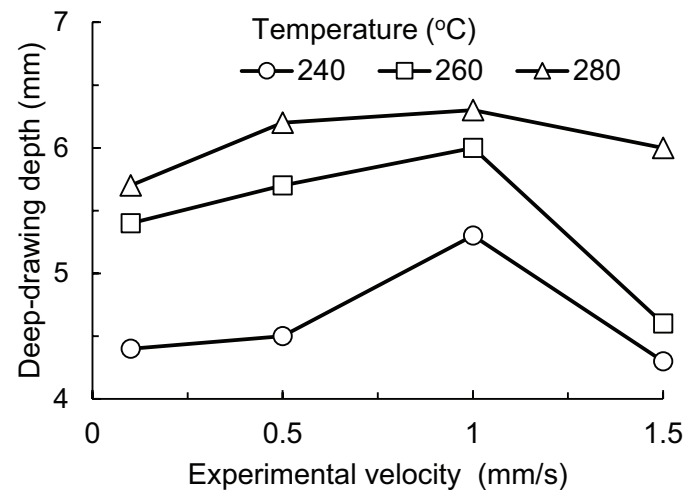


Figure 9: Variation in deep-drawing depth with experimental velocity.

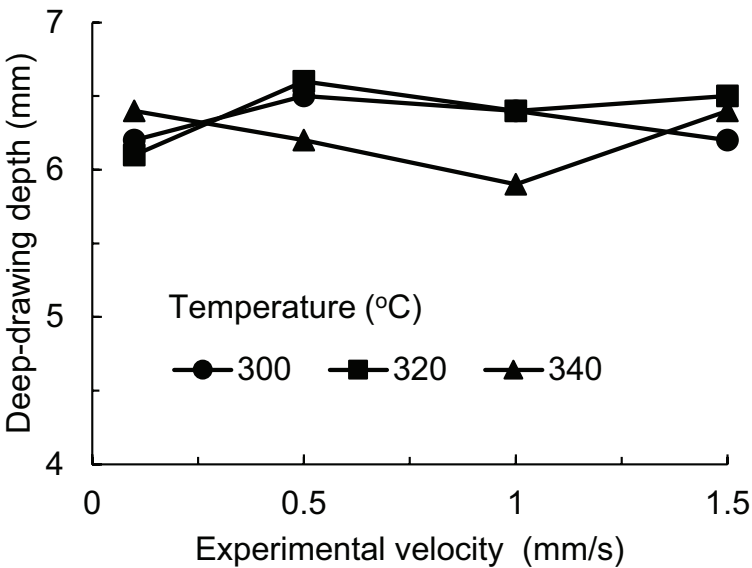


Figure 10: Variation in deep-drawing depth with experimental velocity.

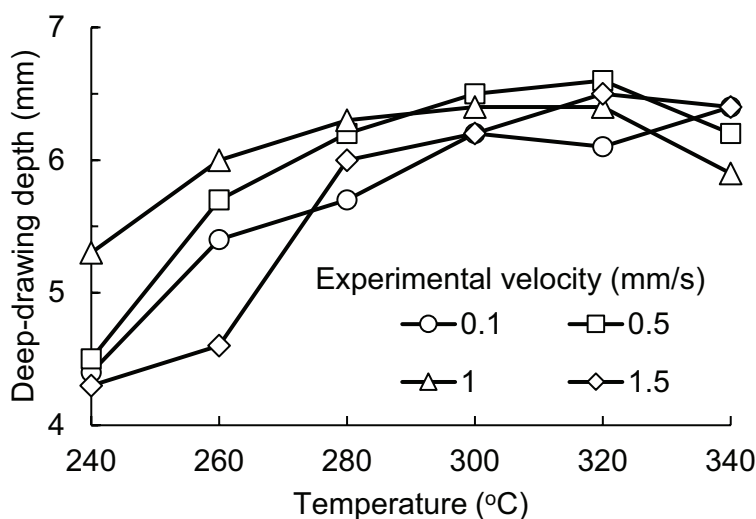


Figure 11: Variation in deep-drawing depth with temperature.

4 NUMERICAL SIMULATION

4.1 Simulation conditions

The material flow, stress distribution and strain distribution in deformed specimens were examined by finite element simulation using DEFORM-3D software to clarify their deep drawability. Figure 12 shows a quarter symmetry model used. The tensile properties obtained in the tensile tests were used as the material properties in the numerical simulation. The other conditions are shown in Table 4.

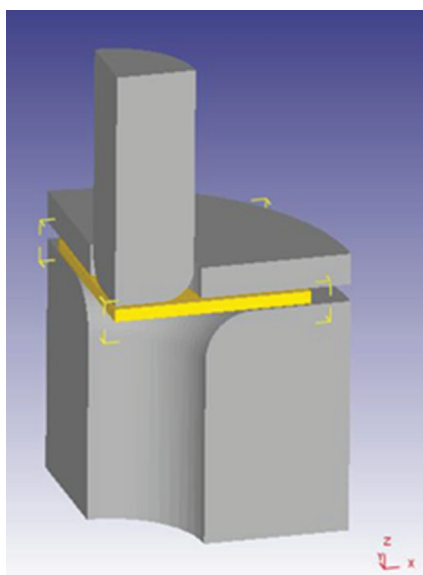


Figure 12: Quarter symmetry model.

Table 4: Numerical simulation conditions.

Material	Rigid-plastic material
Coefficient of friction μ	0.1
Experimental velocity	0.1 mm/s, 0.5 mm/s
Temperature	320°C

4.2 Simulation results

Figures 13 and 14 show the strain distributions at an intermediate depth and the fracture depth for experimental velocities of 0.1 mm/s and 0.5 mm/s, respectively. The maximum deep-drawing depths evaluated by the numerical simulation were 6.3 mm and 5.9 mm for experimental velocities of 0.1 mm/s and 0.5 mm/s, respectively. The maximum deep-drawing depths obtained from the experiments were 6.33 mm and 6.0 mm for experimental velocities of 0.1 mm/s and 0.5 mm/s, respectively. The simulation results were in good agreement with the experimental results. The strain became concentrated on the cup shoulder (punch shoulder), resulting in a fracture there. The locations of crack initiation and propagation in the simulation were also in good agreement with the experimental results.

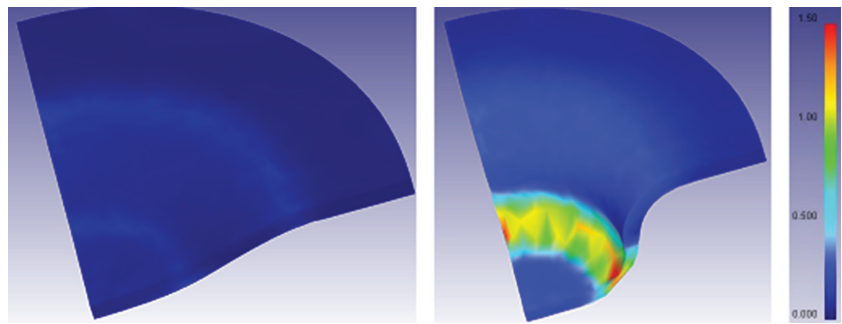


Figure 13: Change in strain distribution from an intermediate depth to the breaking depth.

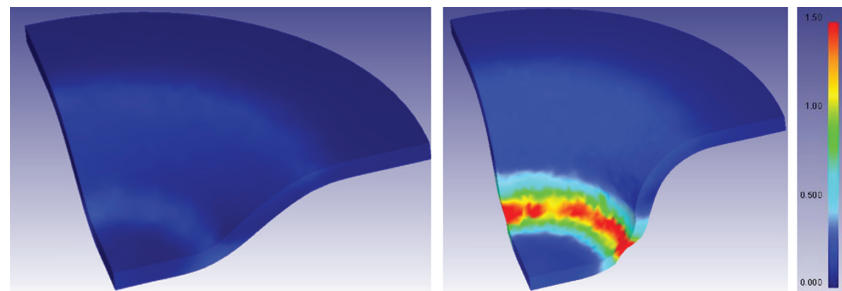


Figure 14: Change in strain distribution from an intermediate depth to the breaking depth.

5 CONCLUSIONS

1. The mechanical properties of flame-retardant AMCa602 magnesium alloy sheets (aluminum, 6.5%; zinc, 0.08%; manganese, 0.32%; calcium, 2.1%) were acquired at different temperatures, and their temperature and velocity dependences were clarified. The flow stress decreased and the ductility improved with increasing temperature.
2. Deep drawability was improved by increasing temperature. The optimum temperature for deep-drawing conditions was found to be 320°C.
3. A numerical simulation of deep drawing was conducted at 320°C by finite element method. The locations of crack initiation and propagation in the simulation were in good agreement with the experimental results. A maximum deep-drawing depth was also obtained in the experiments and simulation.

REFERENCES

- [1] Yoshinaga, H. & Horiuchi, R., Deformation mechanisms in magnesium single crystals compressed in the direction parallel to hexagonal axis, *Transactions of the Japan Institute of Metals*, **4**(1), pp. 1–8, 1963. <https://doi.org/10.2320/matertrans1960.4.1>
- [2] Doege, E. & Droder, K., Sheet metal forming of magnesium wrought alloys—formability and process technology. *Journal of Materials Processing Technology*, **115**(1), pp. 14–19, 2001. [https://doi.org/10.1016/s0924-0136\(01\)00760-9](https://doi.org/10.1016/s0924-0136(01)00760-9)
- [3] Takuda, H., Yoshii, T. & Hatta, N., Finite-element analysis of the formability of a magnesium-based alloy AZ31 sheet. *Journal of Materials Processing Technology*, pp. 89–90, 135–140, 1999. [https://doi.org/10.1016/s0924-0136\(99\)00039-4](https://doi.org/10.1016/s0924-0136(99)00039-4)
- [4] Yoshihara, S., Nishimura, H., Yamamoto, H. & Manabe, K., Formability enhancement in magnesium alloy stamping using a local heating and cooling technique: circular cup deep drawing process. *Journal of Materials Processing Technology*, 142(3), pp. 609–613, 2003. [https://doi.org/10.1016/s0924-0136\(03\)00248-6](https://doi.org/10.1016/s0924-0136(03)00248-6)
- [5] Yoshihara, S., Yamamoto, H., Manabe, K. & Nishimura, H., Formability enhancement in magnesium alloy deep drawing by local heating and cooling technique. *Journal of Materials Processing Technology*, pp. 143–144, 612–615, 2003. [https://doi.org/10.1016/s0924-0136\(03\)00442-4](https://doi.org/10.1016/s0924-0136(03)00442-4)
- [6] Minami, A., Sakamoto, H. & Marumo, Y., Deep drawing formability of the measurement of magnesium sheet metals. *WIT Transactions on Engineering Sciences*, **118**, pp. 1–10, 2017. <https://doi.org/10.2495/cmем170011>